Ultrasonic investigation of the magnetic phase diagram of the quasi-one-dimensional ferromagnet $CsNiF_3$

Benoit Lussier and Mario Poirier
Centre de Recherche en Physique du Solide, Département de Physique, Université de Sherbrooke, Sherbrooke, Québec, Canada J1K 2R1
(Received 8 March 1993)

High-resolution ultrasonic-velocity and attenuation data are used to obtain the magnetic phase diagram of the quasi-one-dimensional ferromagnet $CsNiF_3$. Anomalies in the elastic constant C_{33} and in the ultrasonic attenuation have been observed and related to the three-dimensional ordering of the spins. The phase diagram is obtained for a magnetic field in the basal plane and along the chain axis and for an angular variation of the magnetic field. In the basal plane the exponent β is consistent with the Ising universality class while along the hexagonal axis it is more consistent with the Heisenberg class. A comparison with previous neutron measurements for fields in the basal plane and mean-field predictions along the various directions studied is also provided. Finally, the frequency dependence of the elastic anomalies and the enhancement of the Néel temperature and critical fields will be discussed in relation to domain formation in the paramagnetic phase and to the highly nonlinear behavior of this compound.

I. INTRODUCTION

In recent years hexagonal magnetic ABX_3 compounds have been widely studied both experimentally and theoretically.[1] The quasi-one-dimensional nature of the magnetic interactions leads to a great diversity of structural and magnetic properties of which the magnetic ones have been studied the most. The magnetic phase diagram of these compounds can provide a powerful testing ground for theories of phase transitions and critical phenomena. Among these compounds $CsNiF_3$ is now considered to be the best example of a quasi-one-dimensional ferromagnet. Short-range ferromagnetic correlations along the c-axis chains of Ni^{2+} ions ($S=1$) develop at temperatures below 80 K; the parallel exchange interaction is $J_{\parallel}=20$ K.[2] A large single-ion magnetic anisotropy between directions parallel and perpendicular to the axis, $D\sim 8.5$ K,[2] confines the moments to lie in the hexagonal basal plane. At a temperature $T_N\sim 2.7$ K correlations between the chains build up [$|J_{\parallel}|/|J_{\perp}|\approx 100$ (Ref. 3)] and a phase transition characterized by a three-dimensional ordering of the Ni^{2+} moments occurs. The ferromagnetic character of the spins along the c axis remains and there is an onset of antiferromagnetic ordering in the basal plane. In the absence of an applied magnetic field, basal plane ordering consists of a three-domain structure where the spins are directed along one of the three basal plane crystallographic axes. The effect of applying a magnetic field in the basal plane in a direction perpendicular to one of the spin directions is to increase the size of the domain relative to the other two.[4] A further increase in field strength reduces the amplitude of the long-range order. The critical field above which order is destroyed has been measured as a function of temperature in neutron[4] and magnetization[5] experiments. We are unaware of any values reported for field directions out of the basal plane. In $CsNiF_3$, the importance of relatively strong magnetic dipolar interactions (comparable with exchange coupling) in the basal plane should favor a mean-field description of the phase transition outside a narrow critical region since they tend to suppress critical fluctuations. This has been partly shown to be evident in specific-heat data[3] and in neutron-scattering experiments[6] where a mean-field exponent $\beta=0.5$ was observed. The more precise magnetization data[5] yielded, rather, $\beta=0.34$, consistent with the XY model universality class.

In these magnetic compounds there is an important coupling of the order parameter to the elastic strain tensor which gives interesting elastic properties. In the paramagnetic phase, many elastic constants soften as the temperature is reduced; moreover, anomalies appear at the phase transition and these can be used to map the magnetic phase diagram of the compounds. This has been done, for example, for two quasi-one-dimensional antiferromagnets $CsNiCl_3$ (Ref. 7) and $CsMnBr_3$ (Ref. 8). The elastic properties of $CsNiF_3$ have been studied by many techniques: the vibrating reed by Barmatz *et al.*,[9] Brillouin scattering by Käräjämäki, Taiho, and Levola,[10] ultrasonic propagation and Brillouin scattering by Ganot *et al.*,[11] and ultrasound and thermal expansion by Simpson, Caillé, and Jericho.[12] The large softening of the Young's modulus along the c axis observed by Barmatz *et al.*[9] has never been reproduced in subsequent studies. In all other experiments the elastic constants are found to increase upon cooling from room temperature except C_{44} which softens below 175 K. The only anomaly reported at the phase transition in the literature,[12] except the vibrating reed measurement of Barmatz *et al.*,[9] has been tentatively associated with C_{44}. We will report here that an anomaly is only observed on C_{33}, in contradiction with mean-field predictions.[13] It is then the purpose of the present high-resolution ultrasonic study to examine in detail the behavior of the phase boundary line close to the Néel temperature for different magnetic-field orientations relative to the c axis. For the two main orientations, the deduced exponents β are different and a mean-field description is inadequate; in the basal plane the exponent is consistent with previous magnetization experiments.

We will also emphasize the need to include the nonlinear behavior of this compound to understand the complete phase diagram.

II. EXPERIMENT

The ultrasonic velocity was measured using a pulsed acoustic interferometer, whose operating principle is based on the measurement of the phase difference between the ultrasonic wave and a reference signal.[14] This phase difference Φ is inversely proportional to the ultrasonic velocity V according to the relation,

$$\Phi = \frac{2\pi f L}{V} ,$$

where L and f are, respectively, the sample's length and the frequency of the ultrasonic wave. If the phase difference is maintained constant by means of a computer-controlled feedback loop, then the relative velocity variation is given by

$$\frac{\Delta V}{V} = \frac{\Delta f}{f} + \frac{\Delta L}{L} .$$

One can, therefore, relate the variations in the ultrasonic velocity to the changes in frequency and the changes in length of the sample due to magnetostriction and thermal expansion. Magnetostriction and thermal expansion effects (evaluated using the data of Ref. 12) were neglected as they are at least one order of magnitude smaller than measured velocity variations.

For longitudinal waves propagating along the c axis in the hexagonal symmetry, the changes in the velocity can be related to the changes in the elastic constant C_{33} as follows:

$$\frac{\Delta V}{V} = \frac{1}{2}\frac{\Delta C_{33}}{C_{33}} .$$

Therefore the measured changes in frequency can be directly related to the changes in the elastic constant C_{33}. The ultrasonic attenuation is obtained from the amplitude of the first transmitted pulse at the output of the sample.

The sample used for this experiment measured approximately $2\times7\times17$ mm^3. Its tendency to cleave along the $\{1120\}$ plane facilitated its orientation for acoustic propagation along the c axis [0001]. Parallel faces perpendicular to the c axis were polished to receive longitudinal Y-cut $LiNbO_3$ transducers (30 MHz) bonded to the crystal by a silicone sealant. Longitudinal acoustic waves were generated at 30, 90, 150, 210, and 270 MHz. A precision better than 1 ppm can be obtained using this phase comparison method.

Magnetic-field amplitudes between 0 and 10 T were applied using a superconducting coil. The sample was rotated in the magnetic field using a sensitive gear system for which a precision of 0.1° can be obtained. Because of the large mass of our sample, the absolute value of its temperature could only be determined within ±0.03 K from one experiment to the other. Temperature stability was, nevertheless, obtained within 20 mK using a Si diode for measurements in zero field, while a carbon-glass resistor and a $SrTiO_3$ capacitance were used for measurements in the magnetic field.

III. RESULTS AND DISCUSSION

In order to map out the magnetic phase diagram of ABX_3 compounds from an ultrasonic experiment, one can look for anomalies appearing at the phase transition on the temperature dependence of both the velocity (elastic constant) and the attenuation. These anomalies are subsequently studied as a function of a magnetic field oriented along different directions. For $CsNiF_3$, well-defined anomalies are only observed for longitudinal waves propagating along the hexagonal axis.

A. Magnetoelastic coupling

The relative variation of the elastic constant C_{33} and the attenuation as a function of temperature at different ultrasonic frequencies are, respectively, shown in Figs. 1(a) and 1(b) for zero magnetic field. The data were normalized to their value at 2 K and the curves have been shifted vertically for clarity. Anomalies at the phase transition (2.7 K) are observed in both quantities. Their shape is strongly dependent on frequency over the 30–270 MHz range, a situation which as far as we know, has not been observed before on compounds of the same family.[7,8]

At the highest frequencies (210–270 MHz), the transition is seen around 2.67 K as a slope variation of the elas-

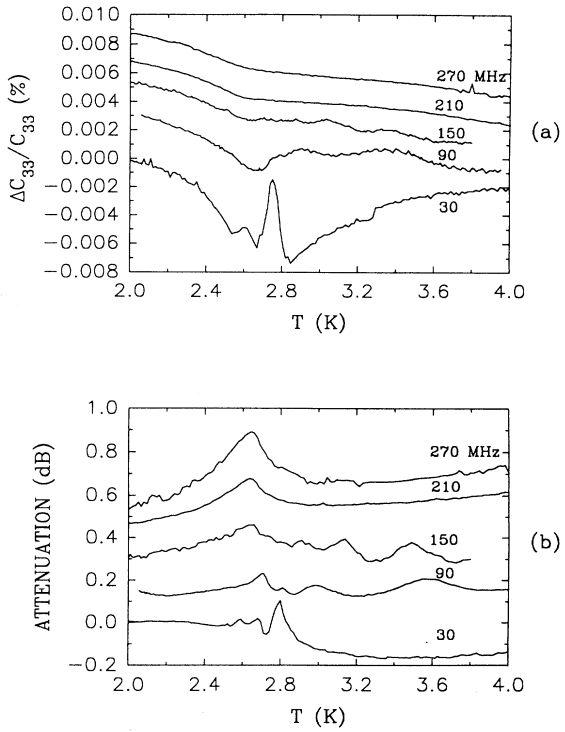

FIG. 1. Relative variation of the elastic constant C_{33} (a) and attenuation (b) as a function of temperature at various ultrasonic frequencies.

tic constant and a peak on the attenuation. As the frequency is lowered the slope variation is changed into a depression of increasing amplitude; the attenuation peak decreases as expected with frequency. On the elastic constant, the minimum of the depression is centered at 2.67 K, the most reported Néel temperature in the literature; we will see in Sec. III B that T_N is higher around 2.77 K where the depression begins. For higher temperatures, and thus in the paramagnetic phase, well-defined thermal oscillations are seen on both the elastic constant and the attenuation: their wavelength increases with temperature but decreases with frequency. These oscillations persist up to 15 K and their origin is not yet understood; they could be related to a domain structure present in the one-dimensional paramagnetic phase. To prevent any obstruction from these oscillations to map out the phase diagram, we will use the high-frequency data (210 MHz) for our study. We have, however, verified that the phase diagrams presented in this paper are not dependent on frequency.

The only similar anomaly observed in an ultrasonic experiment was reported by Simpson, Caillé, and Jericho;[12] they interpreted their data by assuming that they were observing a bar mode at 10 MHz, associated with the elastic constant C_{44}. We have clearly verified for our sample that C_{44} is free from any anomaly over this frequency range. We believe that the observed bar mode was associated with C_{33}; besides, the amplitude of their anomaly at 10 MHz (10^{-4}) is fully consistent with ours at 30 MHz (6×10^{-5}). No thermal oscillations for $T>2.7$ K were reported by these authors.

We thus conclude from our data that the magnetic phase transition around 2.7 K in $CsNiF_3$ produces a variation of the magnetoelastic coupling; this gives a depression on the elastic constant C_{33} whose amplitude is frequency dependent. The exact shape of the anomaly with temperature is dependent on the interaction terms appearing in the magnetoelastic energy and the minimum will not be necessarily centered at T_N. The only prediction known for this elastic constant is a mean-field one made by Plumer and Caillé;[13] they predicted a variation at the transition $\Delta C_{33}/C_{33}\approx2.2\times10^{-6}$, a value smaller by more than one order of magnitude than the measured value. This anomaly will now be studied at a frequency of 210 MHz as a function of the magnetic field to obtain the phase diagram.

B. Magnetic phase diagram

The magnetic phase diagram for the field oriented in the basal plane has been obtained from neutron-diffraction[4] and magnetization experiments.[5] To our knowledge, no experimental investigation of the phase diagram is reported in the literature for orientation of the field along the hexagonal axis or for its angular dependence. Only theoretical mean-field predictions have been proposed by Plumer and Caillé.[13]

1. Magnetic-field oriented in the basal plane

Figure 2 shows the variation of the elastic constant $\Delta C_{33}/C_{33}$ and the attenuation obtained as a function of a magnetic field at fixed temperatures below T_N for a frequency of 210 MHz. The magnetic field is oriented parallel to the basal plane. In Fig. 2(a), as the field is increased, the elastic constant softens, reaches a minimum, and then hardens abruptly; an arrow indicates, at each temperature, the field at which the hardening rate is maximum. This determines the critical field at a fixed temperature, separating the ordered state (three-dimensional antiferromagnetic) at low fields from the paramagnetic state at high fields. The small structure appearing for $H<0.05$ T is likely to be related to monodomain formation.[4] It is useful to note here that at $T=2.66$ K (the most reported Néel temperature is $T_N=2.67$ K) the critical-field value is still 0.15 T; the exact Néel temperature must then be higher, as will be discussed shortly. In Fig. 2(b), the attenuation presents a structure that can be mapped on the variation of the elastic constant. The transition is seen here as a sudden increase of the attenuation and the arrows indicate the critical field determined from Fig. 2(a). The choice of our definition for the critical field is only guided by the occurrence of coherent structures on both the attenuation and the elastic constant variation, since we cannot gauge the exact field dependence of the elastic anomaly; this is an adequate choice which minimizes the error on H_c. The same procedure will be used in subsequent sections.

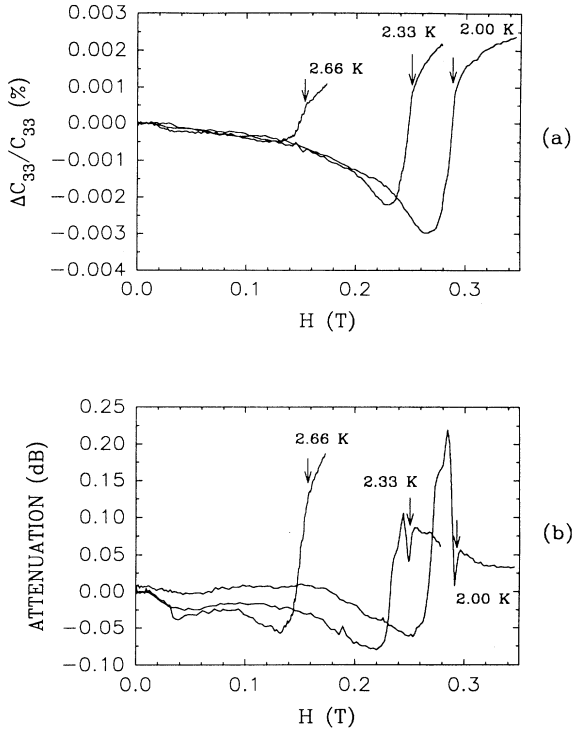

FIG. 2. Relative variation of the elastic constant C_{33} (a) and attenuation (b) at different temperatures as a function of magnetic field for fields in the basal plane at a frequency of 210 MHz.

Similar magnetic-field scans were obtained at different temperatures between 2.0 and 2.8 K: the deduced critical

fields were used to obtain the phase diagram shown in Fig. 3 (diamonds). The diagram is characterized by a slow decrease of the critical field as the temperature is increased from 2.0 K; the decrease rate becomes larger for $T > 2.65$ K and no critical field could be deduced over 2.74 K. This temperature dependence is similar to the one deduced from the neutron-diffraction experiment (circles), except for the field and temperature scales; at 2.0 K, our critical field is near 0.29 T when the neutron value is just over 0.21 T; moreover, the Néel temperature deduced from magnetization data[5] is 2.665(8) K while ours is likely to be 2.77(1) K, a difference larger than the precision on the absolute value (0.03 K). This discrepancy in scales will be discussed shortly.

In Fig. 3 we have also added the results of a mean-field prediction (using $T_N = 2.77$ K) as proposed by Plumer and Caillé;[13] even very near T_N, disagreement with experimental data is observed. We remind the reader that mean-field theory works nicely to explain the phase diagram deduced from ultrasonic data in other ABX_3 compounds. At the boundary between the paramagnetic and the ordered phases the critical field H_c should scale as the zero-field order parameter S_0;[13] we can thus write $H_c \sim (T_N - T)^{\beta}$ for the critical behavior. This expression, used for $T > 2.6$ K, yielded a best fit over the complete temperature range as is shown in Fig. 3. The parameters are $T_N = 2.77 \pm 0.01$ K and $\beta = 0.31 \pm 0.01$. This exponent β is smaller than the value deduced from magnetization,[5] $\beta = 0.34 \pm 0.3$, but considering the error on this last value, it seems to be consistent with the Ising universality class.

Now we have to ask the question why, in the ultrasonic experiment, the low-temperature critical field and the Néel temperature values are higher. The answer is related to the recent history of the sample. These ABX_3 compounds are highly hygroscopic and they are always kept under dry atmosphere to maintain their intrinsic quality. Our crystal was excellent; a nice transparent green single crystal having a minimum of defects, mainly cleavage planes along the hexagonal axis. Moreover, the crystal had never been subjected to high magnetic fields before the ultrasonic study. The first experiment has been performed with the magnetic field in the basal plane and the phase diagram obtained at 30, 90, and 210 MHz is shown in Fig. 4; as said before, the diagram is frequency independent and very similar to the neutron-diffraction data.[4] The next experiment was to rotate the sample to produce an angle of 30° between the basal plane and the field direction. When the field was increased up to 10 T, an important torque was surprisingly exerted on the sample in the paramagnetic phase so as to move the sample from its initial direction. To proceed further with the experiment, we had to modify the sample holder to prevent any other movement of the sample during the field scan, then realign the crystal to maintain the field in the basal plane and reobtain the previous phase diagram. The result was very surprising; a similar diagram, but with enhanced critical field and Néel temperature values as shown at 210 MHz in Fig. 4. Subsequent thermal (2–300 K) and magnetic cyclings (0–10 T) did not modify the diagram. Since the crystal was always kept in low helium-gas pressure and no mechanical stress was applied, this enhancement is likely related to the application of a high field, possibly modifying the magnetic microstructure. A small hysteresis is, indeed, observed at the phase transition indicating the persistence of domains, while we thought that a small field had produced a monodomain. The thermal oscillations observed in the paramagnetic state could be related to this domain structure. How exactly is this microstructure modified by the application of a high magnetic field is left as an open question. In this paper the critical fields were always measured for increasing magnetic fields; the values ob-

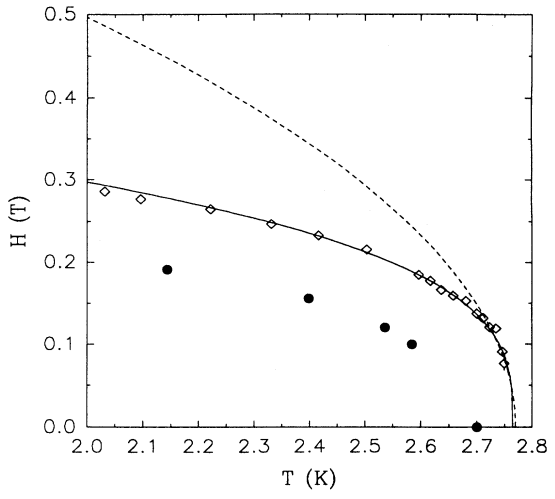

FIG. 3. Phase diagram obtained at 210 MHz (diamonds) for fields in the basal plane; comparison with mean-field predictions (dotted line) and neutron data (circles). Solid line was obtained from a least-squares fit (see text).

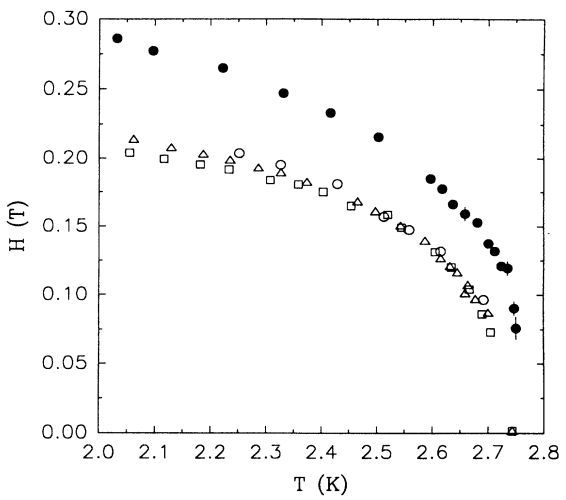

FIG. 4. Phase diagram obtained for fields in the basal plane: before magnetic cycling at 30 (hollow circles), 90 (hollow squares), and 210 MHz (hollow triangles); after magnetic cycling at 210 MHz (filled circles).

tained for decreasing fields are a little smaller but they are still higher than the neutron data.

2. *Magnetic-field oriented parallel to the hexagonal axis*

For the field oriented parallel to the hexagonal axis, we present in Fig. 5 the elastic constant variation and the attenuation as a function of field at a fixed temperature of 2.0 K. Now the field scale extends up to 2.6 T. In Fig. 5(a) the attenuation increases with field in a monotonic way; at ~2 T, we observe a small local maximum likely related to the phase transition. The elastic constant shown in the same figure softens with increasing field and the phase transition may be seen as a small change of slope at ~2 T. An enlarged region is presented in Fig. 5(b) to better appreciate the behavior of both parameters; an arrow indicates the critical field corresponding to the onset of the phase transition. For all temperatures between 2.0–2.8 K the observed anomaly was similar and field scans up to 10 T did not reveal other structures that could be related to the transition.

We present in Fig. 6 the phase diagram deduced from the measured critical field at different temperatures. To our knowledge, this diagram has never been reported experimentally. The overall dependence of the critical field on temperature is similar to the previous phase diagram. At first, the critical field decreases slowly with increasing temperature and then more rapidly for $T > 2.65$ K. Evidently, the critical behavior near the Néel temperature is not mean field and, if we use a similar expression as before to relate the critical field to the order parameter, we obtain a best fit for $T > 2.6$ K with parameters $T_N = 2.80 \pm 0.01$ K and $\beta = 0.37 \pm 0.01$. Considering the imprecision of the absolute value of the temperature from one experiment to the other (0.03 K), the Néel temperature is consistent with the previous one. The exponent β is, however, larger and more in agreement with the Heisenberg universality class; a temperature shift of 0.02 K to reconcile the Néel temperatures does not modify the exponent. The low-temperature critical-field values are also different being eight times larger for this particular orientation, a value much smaller than the expected one based on the ratio $D/J_\perp \sim 30$. In the basal plane, the magnetic field competes with the interchain exchange constant $J_\perp$, which is of the order of 0.28 K or 0.28 T;[3] this explains, qualitatively, the observed critical field (0.29 T) for this orientation. When the field is oriented perpendicular to this plane, the field is rather in competition with the single-ion magnetocrystalline anisotropy $D = 8.5$ K (Ref. 2) or approximately 8.5 T. For this field orientation, the observed value, 2.3 T, is thus much smaller than expected.

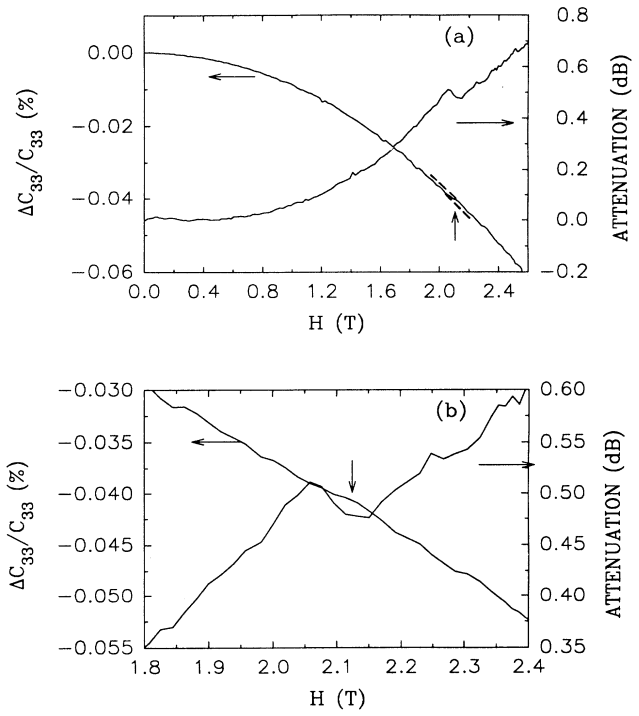

FIG. 5. Relative variation of the elastic constant C_{33} and attenuation (a) at 2 K as a function of magnetic field for fields along the chain axis at 210 MHz; graph (b) is an enlargement. The dashed lines are guides for the eye.

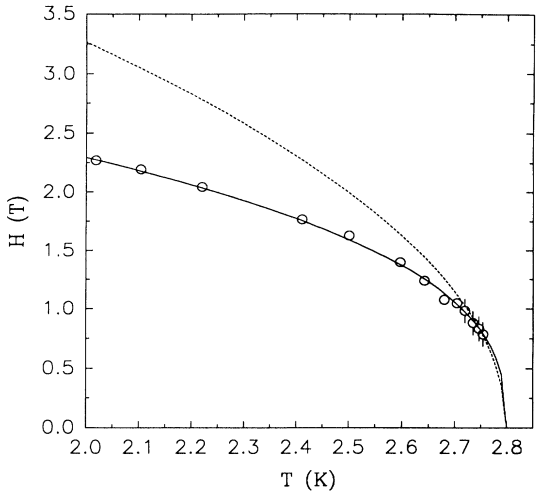

FIG. 6. Phase diagram obtained at 210 MHz (circles) for fields along the chain axis; comparison with mean-field predictions (dotted line). Solid line was obtained from a least-squares fit (see text).

3. *Angular dependence of the phase diagram*

The angular dependence of the magnetic phase diagram can also provide a complementary view of the competing magnetic interactions and excitations present in the studied crystal. This has been done, for example, for the antiferromagnet $CsMnBr_3$ (Ref. 8) where mean-field theory fits very well not only the phase diagram but also its angular dependence.

We show in Fig. 7 the elastic constant and attenuation data obtained as a function of the magnetic field at a fixed temperature of 2.0 K for different field orientations; the angle is measured relative to the basal plane. For the

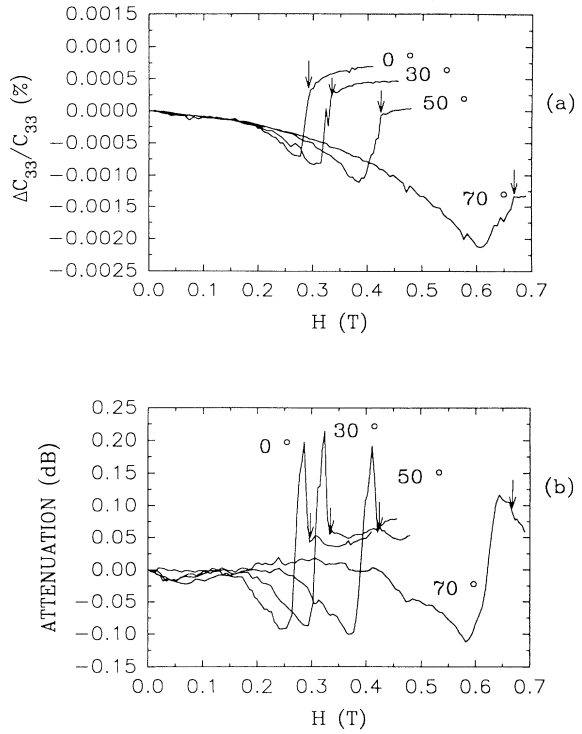

FIG. 7. Relative variation of the elastic constant C_{33} (a) and attenuation (b) at 2 K as a function of the orientation of the magnetic field (0° being the basal plane and 90° the c axis).

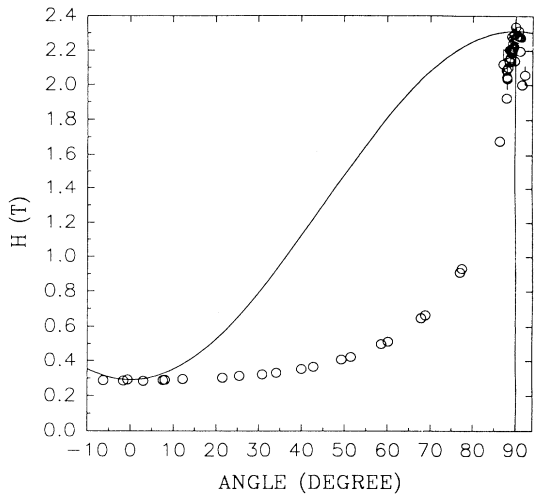

FIG. 8. Angular dependence of the phase diagram at 2 K and 210 MHz (circles); comparison with mean-field predictions (solid line).

elastic constant [Fig. 7(a)], the critical field is easily identified by the discontinuity indicated by the arrow; on the attenuation, the phase transition produces a peaked structure whose onset is also indicated by an arrow. This critical field at 2.0 K has been followed for many angles between 0° and 90°; its angular variation is given in Fig. 8. In the same figure we have plotted the mean-field prediction in order to fully appreciate the particular angular dependence observed for this compound. When the field deviates from the plane direction (0°), the critical field barely increases; it is only for $\theta > 45°$ that the critical field increases more rapidly. The increase is particularly steep beyond 80°, the maximum value of 2.3 T is obtained over a very narrow range of angles. The same angular dependence was obtained for higher temperatures (2.3 and 2.6 K) with consequently smaller critical fields.

Such a peculiar angular dependence has not been observed yet in other crystals; as said previously, antiferromagnetic compounds of the same family seem to be well described by mean-field theory. One may ask the question as to why is it different for the ferromagnet $CsNiF_3$. Is this angular behavior observed in other magnetic properties? Seitz and Benner[15] have studied the angular dependence of the nuclear relaxation rate T_1^{-1} in the paramagnetic phase; they have obtained a dependence very similar to the one observed in the ultrasonic experiment. According to Plumer,[16] one can invoke simple phenomenological arguments to relate the relaxation rate to the order parameter and, therefore, to the critical field. Following Seitz and Benner, this peculiar angular dependence may be fitted by a model which includes magnon and soliton contributions. It has been shown in the literature that the nonlinear behavior of this compound must be considered to explain the static and dynamic magnetic properties. This must also be the case for the magnetoelastic coupling. Contrary to the other compounds, the anomaly observed on the elastic constant C_{33} is frequency dependent and its amplitude is much larger than the prediction of mean-field theory. Moreover, thermal oscillations appear on both the elastic constant and attenuation below 150 MHz in the paramagnetic phase. We thus believe that more elaborate models incorporating nonlinear excitations are needed to explain the peculiar magnetoelastic coupling and the critical behavior of the complete phase diagram.

IV. CONCLUSION

We have presented in this paper a complete magnetic phase diagram of the quasi-one-dimensional ferromagnet $CsNiF_3$, using an ultrasonic experiment. The phase diagram was obtained from the observation of anomalies on the velocity and attenuation of longitudinal ultrasonic waves propagating along the hexagonal axis. The shape of these anomalies were frequency dependent but the deduced phase diagram was not. For the magnetic field oriented in the basal plane, the diagram is very similar to the one deduced from neutron-diffraction and magnetization experiments but the critical fields and the Néel temperature are somewhat higher. The universality class is likely to be Ising, in agreement with ferromagnetic planes coupled antiferromagnetically. The phase diagram with field oriented along the hexagonal axis is reported and is somewhat different from the other one; the exponent agrees with a Heisenberg universality class. The critical field value is eight times larger, a value much smaller

than the expected single-ion anisotropy to the interchain exchange constant ratio. The angular dependence of the critical field was also obtained and it confirmed the inadequacy of mean-field theory to explain the critical behavior of this ferromagnet. The experiments seem to indicate that the nonlinear behavior of this compound should be taken into account to fully understand the peculiar magnetoelastic coupling and the deduced magnetic phase diagrams. Finally, hysteretic effects, enhancement of the critical field, the Néel temperature, and the particular shape of the phase diagram near T_N may suggest that the phase transition could be slightly first order.

ACKNOWLEDGMENTS

The authors wish to thank M. L. Plumer and A. Caillé for stimulating discussions and M. Castonguay for technical assistance. Financial support was provided by The Natural Sciences and Engineering Research Council of Canada (NSERC) and the Fonds pour la Formation de Chercheurs et Aide à la Recherche du Québec (FCAR).

[1]For $CsNiF_3$, see M. Steiner and J. Villain, Adv. Phys. **25**, 8 (1976); H. J. Mikesha and M. Steiner, *ibid.* **40**, 191 (1991).
[2]C. Dupas and J. P. Renard, J. Phys. C **10**, 5057 (1977).
[3]J. V. Lebesque, J. Snel, and J. J. Smit, Solid State Commun. **13**, 371 (1973).
[4]M. Steiner and H. Dachs, Solid State Commun. **14**, 841 (1974).
[5]M. Steiner, Phase Transitions **1**, 269 (1980).
[6]M. Steiner and H. Dachs, Solid State Commun. **9**, 1063 (1971).
[7]M. Poirier, A. Caillé, and M. L. Plumer, Phys. Rev. B **41**, 4869 (1990).
[8]M. Poirier, M. Castonguay, A. Caillé, M. L. Plumer, and B. D. Gaulin, Physica B **165-166**, 171 (1990).
[9]M. Barmatz, L. R. Testardi, M. Eibschütz, and H. J. Guggenheim, Phys. Rev. B **15**, 4370 (1977).
[10]E. Käräjämäki, R. Taiho, and T. Levola, Phys. Rev. B **25**, 6474 (1982).
[11]F. Ganot, C. Dugautier, P. Moch, and J. Nouet, Solid State Commun. **29**, 51 (1979).
[12]A. M. Simpson, A. Caillé, and M. H. Jericho, Solid State Commun. **64**, 111 (1987).
[13]M. L. Plumer and A. Caillé, Phys. Rev. B **37**, 7712 (1988).
[14]G. Gorodetshy and I. Lachterman, Rev. Sci. Instrum. **52**, 1387 (1981).
[15]H. Seitz and H. Benner, Z. Phys. B **66**, 485 (1987).
[16]M. L. Plumer (private communication).